

Channel Estimation for Short Range Wireless Sensor Network

F.Darbari, I. McGregor, G. Whyte, R.W.Stewart, I. Thayne

DSP Enabled Communications Group
Department of Electronic and Electrical Engineering
University of Strathclyde
16 Richmond Street, Glasgow, UK, G1 1XW
Email: faisal@eee.strath.ac.uk

Keywords: Digital Sampling Scope (DSS), Line of Sight (LOS), Non Line of sight (NLOS), Root Mean Square (RMS), Weak Signal (WS).

Abstract

This paper investigates the channel parameters (time dispersive properties) for the novel idea of tiny communicators called ‘specks’. These tiny devices are limited with power so a clear idea of the channel impairment is mandatory for the design of onboard DSP. In order to facilitate the design, measurement of the impulse response characteristic has been investigated through different media and antennas. The paper investigates the measured impulse response and statistical properties of amplitude variations for individual impulses for distances of around 10cm in addition to power delay profile, path loss, mean excess delay, root mean square delay, coherence bandwidth, and their impact on system design. The narrowband model has been used to predict the path loss of the channel and extent of coverage of the transmitting speck. The wide band channel sounding has been done to investigate the impulse response parameters such as delay spread, which is used to compute several secondary statistics like coherence bandwidth and data rate.

1 Introduction

Speckled Computing [9] is a collaborative project between five universities in Scotland. The consortium has a vision of designing tiny transceivers of size 1 x 1 x 1 mm for communicating at a range of approximately 10cm. These tiny grains of semiconductors will produce an ad-hoc wireless network capable to be used in variety of military and commercial applications. These tiny grains are fully capable of sensing and processing data with some state of the art onboard DSP and processing technology. Each Speck will be autonomous, with its own captive, renewable energy source. These specks are designed for low power however; each one of them will be capable of optical and radio frequency (RF) communication. The combination of hundreds of such specks will form a very long chain of tiny transceivers called a specknet.

The development of first generation RF based prototype with an initial size of 5 x 5 x 5 mm nodes is well under way. The size of the speck has put a tight constraint on the power

budget and since the specks will be placed on different materials a channel model is required that would help in the design of various physical layer issues, which are critical for system design.

This paper presents a study of wireless channel estimation of these tiny transmitters operating at 2.4-GHz ISM band and investigates various channel parameters that depend upon the scenarios where the specks will be placed. In order to facilitate the design, measurement of the impulse response characteristic has been made through different antennas. The study encompasses the effect of different materials on the above mentioned parameters (since the specks will be placed on different materials) besides estimating noise and interference on channel bandwidth.

2 Research Methodology

The research is based on narrow and wideband sounding technique. Since narrowband measurements are unable to resolve the multipath components in time domain, they are only used to compute the channel path loss. These findings are also termed as long term fading. In order to investigate the small scale fading and to determine the channel impulse response, measurements have been carried out in both time and frequency domain. In the time domain a narrow Gaussian impulse has been sent through wide band (directional and non directional) antennas. The results obtained have been compared with frequency domain channel sounding technique in which the channel scattering parameters (S21) have been computed through a Vector Network Analyzer (VNA). The received signal power at the receiver with a separation distance d is given by [6, 8].

$$P_r(d) = P_l(d) + P_s(d) + P_e(d) + Noise \quad (1)$$

The received signal is affected by the parameters mentioned in Equation (1). The large scale variation $P_l(d)$ (Equation 1) of the received signal depends upon the distance and path loss exponent (d^n). The path loss exponent dictates the rate of decrease in signal strength and it mainly depends upon distance, frequency and environment. The small scale fading components $P_s(d)$ of the received signal generally vary with distances as small as the wavelength of the transmitted signal

and will depend on the multipath component. The shadowing $P_\sigma(d)$ (Equation 2.1) is a zero mean Gaussian random variable and depends on the material and the environment on which the specks will be placed. The receiver sensitivity has been affected by the noise threshold and depends on receiver bandwidth and operating environment. All these factors are discussed in detail in the section below. The measurement set up is shown in the Figure (1).

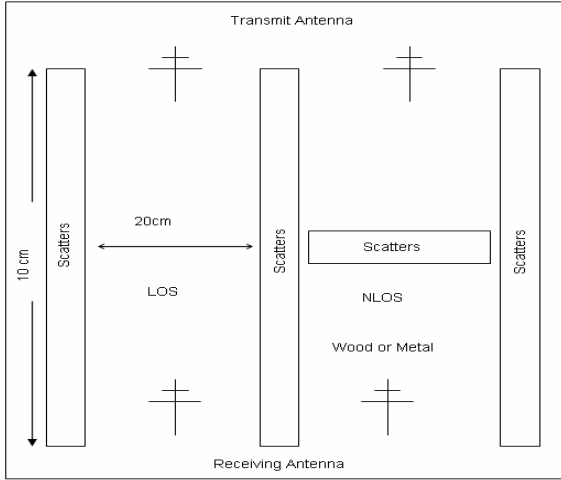


Figure 1: Measurement setup

2.1 Large Scale Fading Effects

Narrow band channel sounding has been done to investigate the large scale fading effect, which is generally referred to as path loss. The path loss (or spreading loss) in free space (LOS Environment) is not frequency dependent [8]. Frequency dependence can only be taken into account when considering the received power due to the antennas used but not for path loss in case of LOS or free space propagation. Currently, there is no clear consensus on the dependence of path loss on frequency excluding antenna effects [4]. Antennas have their power flux density varying with $1/d^2$ [8]. The received power $P_r(d_0)$ has been measured at some reference distance (d_0) to capture the frequency dependence [8] due to the antenna effect by using Equation (2).

$$p_r(d) \text{ (dBm)} = \bar{p}_r(d_0) - 10n \log_{10} \left(\frac{d}{d_0} \right) + x_\sigma \quad (2)$$

To measure average path loss with distance, a single tone at 2.45 GHz has been transmitted through different antennas and materials. A total of five readings are taken with a transmitted tone of 0 dBm and are averaged out. The experiment setup consists of antennas mounted on a stand at a separation distance of 10cm, with scatters placed at right angle to the direction of the transmission as shown in Figure (1). The system is first calibrated to cater for any cable and connector losses. The reference measurements have been made in the far field area of the antennas so that near field effect does not alter the reference path loss. The path loss values have been

measured with increasing distance and the MMSE criteria has been used to compute the mean path loss exponent n [6] for different environments. The measured path loss values in LOS/NLOS environment for materials like wood and metal are shown in Figure (2) and (3). The standard deviation about the mean has been calculated and could be added to simulate the random shadowing effect (x_σ) as shown in Table (1) and (2).

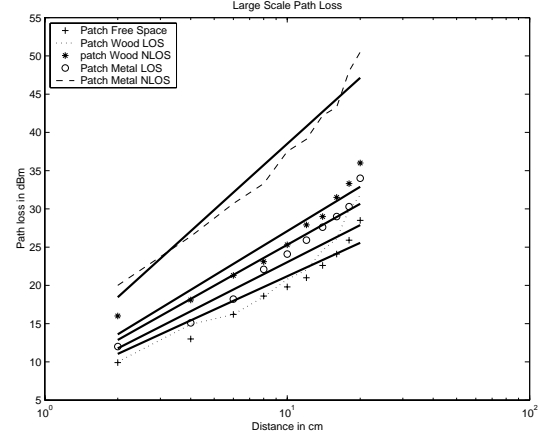


Figure 2: Average path loss for Patch Antenna

S/No	Environment	Path Loss [n]	Standard Deviation [dB]
1	LOS Free Space	1.4	1.2
2	Wood LOS	1.6	1.6
3	Wood NLOS	2.1	2.1
4	Metal LOS	1.8	1.9
5	Metal NLOS	2.8	1.7

Table 1: Large Scale Path Loss Parameters for Patch Antenna

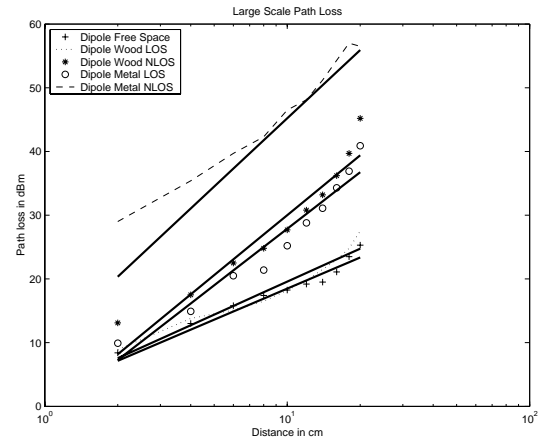


Figure 3: Average path loss for Dipole Antenna

Dipole Antenna			
S/No	Environment	Path Loss [n]	Standard Deviation [dB]
1	LOS Free Space	1.6	1.0
2	Wood LOS	1.7	1.3
3	Wood NLOS	2.4	2.3
4	Metal LOS	2.1	2.2
5	Metal NLOS	3.3	2.8

Table 2: Large Scale Path Loss Parameters for Dipole

The slope of the line is 10n dB/decade [6] with the value of n depending upon the environment. The average value of n (path loss) for wood is 1.95 and for metal are 2.5 as calculated from the Table (1) and Table (2).

The point relating to the path loss can be explained by comparing some important antenna parameters. The patch antenna has a higher directivity [1] than the dipole. This means that the radiation pattern for the patch is more focused in the LOS than the dipole. Higher directivity also means that the gain of the antenna is greater, as gain is directly proportional to directivity [5]. The variance in case of omni directional antenna would certainly be more as compared to the directional antenna as shown in Table (1) and (2). This is because the multipath effect is more in case of non directional antennas as compared to the directional antenna.

In the case of metals the higher value of path loss factor [n] is an indication that there is a phase reversal when the conducting material is placed too close to the antenna which results in destructive interference. The average decrease in signal strength and power estimation equations are given in Table (3) and (4).

S/No	Material	Path Loss [dBm]/cm	Estimation Equation
1	Free Space	0.81	-13.6 - 14 Log(d/3)
2	Wood LOS	0.82	-15.6 - 15 Log(d/3)
3	Wood NLOS	1.19	-17.0 - 21Log(d/3)
4	Metal LOS	0.98	-16.0 - 17Log(d/3)
5	Metal NLOS	1.48	-23.5 - 28Log(d/3)

Table 3 Average Path Loss and Power Estimation Equation for Patch Antenna

S/No	Material	Path Loss [dBm]/c m	Estimation Equation
1	Free Space	0.9	-13.6 - 16 Log(d/5)
2	Wood LOS	0.95	-14.4 - 17 Log(d/5)
3	Wood NLOS	1.0	-21.2 - 23Log(d/5)

4	Metal LOS	0.99	-19.0 - 21Log(d/5)
5	Metal NLOS	1.89	-36.4 - 30Log(d/5)

Table: 4 Average Path Loss and Power Estimation Equation for Dipole Antenna.

2.2 Small Scale fading Effects

To investigate the channel impulse response a Gaussian impulse of 50 picoseconds in duration (resulting in a spatial resolution of 1.5cm) has been sent through a wide band Vivaldi (directional radiation patterns) and Cpw-Monopole antenna (Omni directional radiation pattern). The width of the pulse is inversely proportional to the bandwidth, and it determines the multipath resolution i.e. the minimum differential path delay between individual resolvable multipath components [4]. The period of the periodic Gaussian impulse has been chosen to be greater than the maximum delay spread so that the entire multipath will be available during the silence period. The measurement system used to obtain the pulse response is shown in Figure (4).

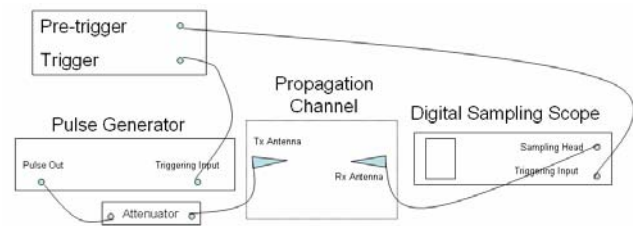


Figure 4: Block diagram of the experimental setup.

The transmitted pulse has been fed to a variable attenuator that provides the safety margin to the digital sampling scope. The whole test bench has been calibrated to compensate for the attenuation losses by first taking the direct measurement between the transmitter and the receiver with high precision cables. The propagation delay between the connecting cables has been calculated and compensated in the measurement procedure so that all multipath have an absolute delay reference. The impulse has been sent through a wide band Vivaldi antenna (with directional radiation pattern) having bandwidth of approximately 10 GHz as shown in Figure (6). The transmitted and received signal has been fed to a high resolution digital sampling oscilloscope. The received signal has been sampled with a time resolution of 2.5 picoseconds. The sampled transmitted and received signal has been stored in a text file in the form of voltage as a function of time. The stored sampled values have been treated as a sampled impulse response for further processing. The synchronization of the transmitter and the receiver has been achieved by triggering the oscilloscope through a cable connection with a sync output of the pulse generator. The transmitting and receiving antennas have been placed at the same height on a test bench for measurement in free space and then on different medias

(wood, metal etc) for channel estimation. During the measurement procedure the movement in the near vicinity has been kept to the minimum and multiple readings are taken to get reasonable channel parameters.

The digital sampling scope is only capable of capturing a certain numbers of samples (depending upon the buffer size) in a measurement scan and the observation window should be comparable with the multipath delay. The current measurement set up of the scope has been set to a buffer size of 4000 samples and sampling interval of 2.5 picoseconds (sampling frequency of 400 GHz) that results in an observation window of 10 ns. This is well above the simulated and measured delay profile of the channel. The whole idea is to transmit the impulse with antennas having directional and non directional radiation patterns.

The received signal power delay profile has been averaged to 10x through the DSS to improve the signal to noise ratio and then is used to compute the time dispersive parameters of the channel. The computed power delay profile has been normalized and the delay calculation is based on the threshold set to 20dBm. The plot in Figure (5) shows the transmitted and the received signal through Vivaldi antenna. The received signal $p(\tau_\kappa)$ spreads in time as compared to the transmitted signal because of the combined effect of antenna and propagation medium. Several secondary channel parameters have been computed from the power delay profile $p(\tau_\kappa)$.

- Mean excess delay [6], which is the first moment of the power delay profile, is defined by Equation (3).

$$\bar{\tau} = \frac{\sum_{\kappa} a_{\kappa}^2 \tau_{\kappa}}{\sum_{\kappa} a_{\kappa}^2} = \frac{\sum_{\kappa} p(\tau_{\kappa}) \tau_{\kappa}}{\sum_{\kappa} p(\tau_{\kappa})} \quad (3)$$

- RMS delay spread [6] is the square root of the second central moment of the power delay profile and is given by Equation (4)

$$\sigma_{\tau} = \sqrt{\bar{\tau}^2 - (\bar{\tau}^2)} \quad (4)$$

Where

$$\bar{\tau}^2 = \frac{\sum_{\kappa} a_{\kappa}^2 \tau_{\kappa}^2}{\sum_{\kappa} a_{\kappa}^2} = \frac{\sum_{\kappa} p(\tau_{\kappa}) \tau_{\kappa}^2}{\sum_{\kappa} p(\tau_{\kappa})} \quad (5)$$

Figure (6) represents the frequency spectrum of the transmitted and received signal and indicates the bandwidth of the antennas.

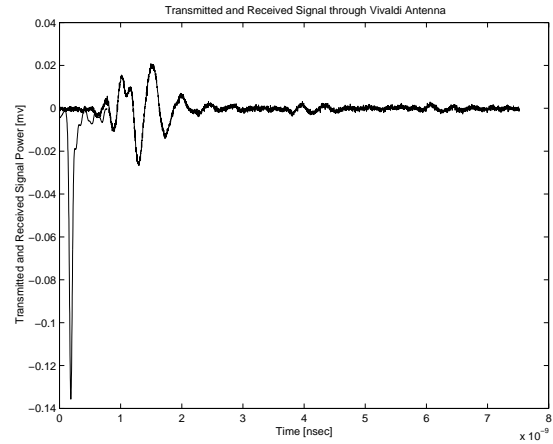


Figure 5: Transmitted and Received Signal

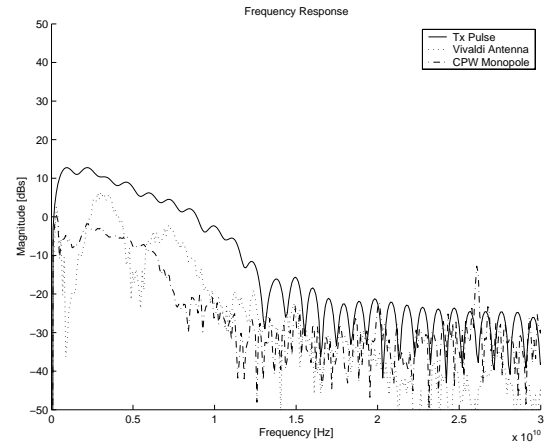


Figure 6: Spectrum of the Transmitted and Received Signal

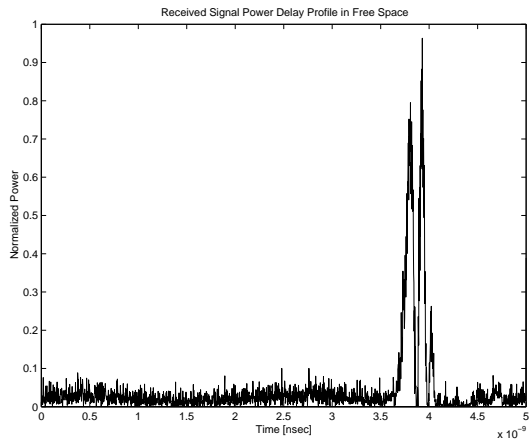


Figure 7: Power delay profile for free space- Monopole

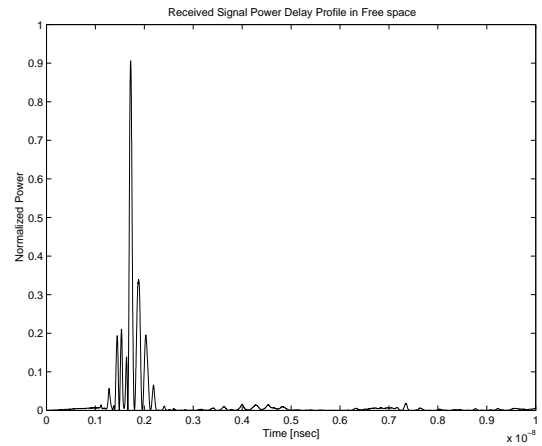


Figure 8: Power delay profile for free space- Vivaldi

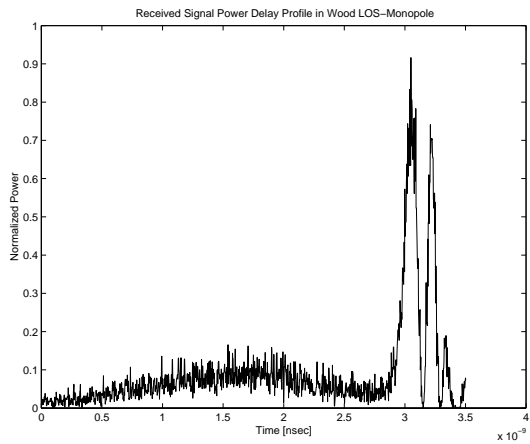


Figure 9: Power delay profile in wood LOS- Monopole

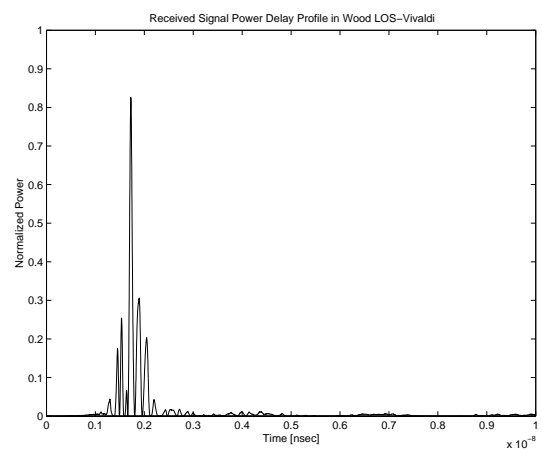


Figure 10: Power Delay Profile in wood LOS, Vivaldi

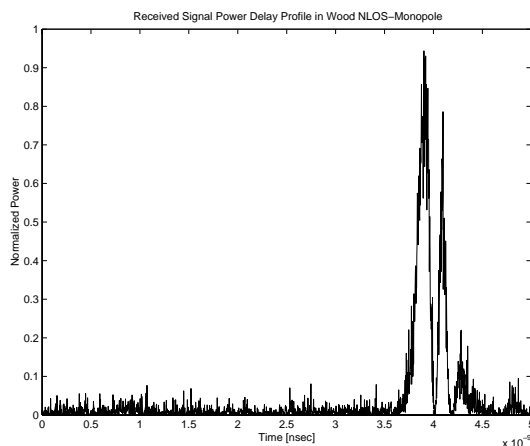


Figure 11: Power Delay Profile in wood-NLOS, Monopole

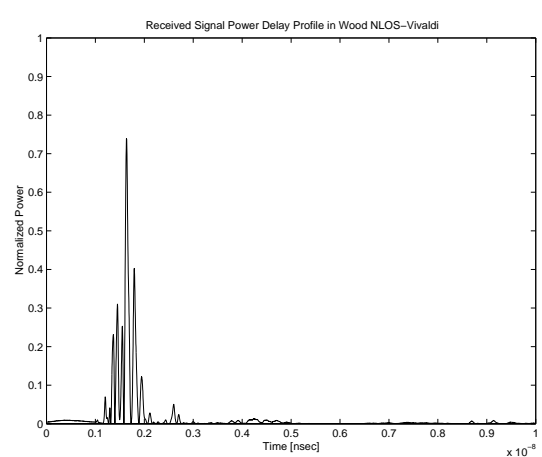


Figure 12: Power Delay Profile in wood-NLOS, Vivaldi

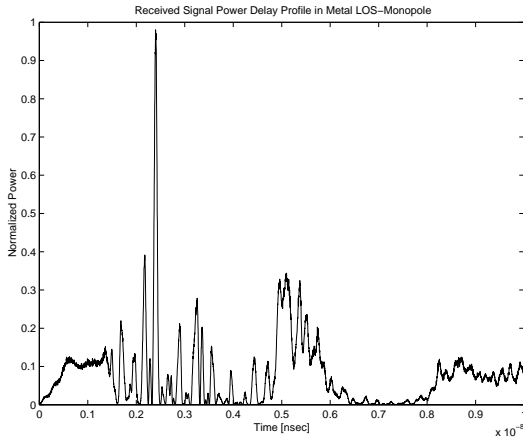


Figure 13: Power Delay Profile in metal LOS, Monopole

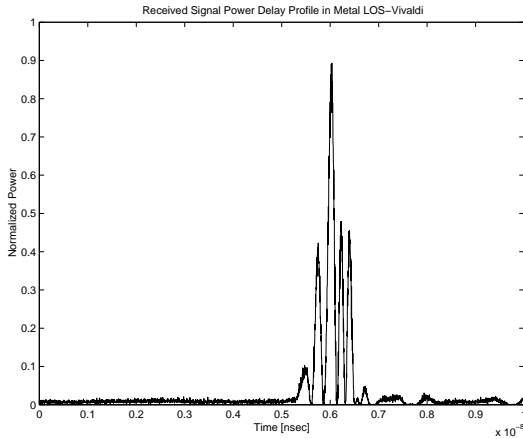


Figure 14: Power Delay Profile in metal LOS, Vivaldi

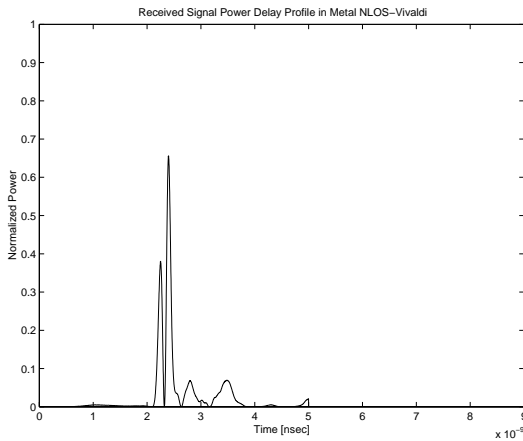


Figure 15: Power Delay Profile in metal NLOS, Vivaldi

The idea is to estimate the coherence bandwidth of channel which is the statistical measure of the range of frequencies on which the channel response is essentially flat, that mean the channel will pass all spectral components with essentially equal gain and linear phase. If the frequency correlation function is set to be 0.5 then the reading of the coherence

bandwidth are reflected in Table (5) and (6).

Monopole	Free Space	Wood LOS	Wood NLOS	Metal-LOS	Metal NLOS
Mean Excess Delay [ns]	0.221	0.289	0.398	2.947	WS
RMS Delay Spread[ns]	0.093	0.119	0.131	1.651	WS
Coherence Bandwidth [MHz]	2150	1680.6	1526.7	121.2	WS

Table: 5 Secondary Channel Statistics for Monopole Antenna

Vivaldi	Free Space	Wood LOS	Wood-NLOS	Metal-LOS	Metal NLOS
Mean Excess Delay [ns]	0.196	0.106	0.20	2.1	WS
RMS Delay Spread[ns]	0.065	0.061	0.07	1.21	WS
Coherence Bandwidth [MHz]	3076.9	3278.8	2857.1	165.2	WS

Table: 6 Secondary Channel Statistics for Dipole Antenna

The first prototype of the speck has a transmission bandwidth of approximately 400 KHz. Since the bandwidth of the transmitted signal is well within the channel coherence bandwidth the channel is considered to be a flat faded channel. This causes deep fades in the transmitted signal and would mean more power is required to compensate for the required bit error rate. Secondly since the coherence bandwidth of the channel is well within the channel bandwidth, the system does not need an equalizer at the receive side.

The received signal in the case of NLOS is weak, as shown in Figure (15) and in Tables (5) and (6). This is because the skin depth, or characteristic depth of penetration of the metal and is defined in [5]. The amplitude of the signal in the conductor decay by an amount (1/e or 36.8%) after travelling one skin depth [5]. For stainless steel this is 9.7 micrometers at 2.45 GHz. Since the separation plate used in our experiment is more than the skin depth the received signal strength drops to negligible. This brings us to a conclusion that if specks are placed with metal between them the decay in signal power is more in non directional antennas as compared to directional with metal of same skin depth. Also the scattering of the signal components is more in metal (as shown in Table (5) and (6)) as compared to wood or free space.

In a wireless channel one of the major degrading factors is the Inter Symbol Interference (ISI) which will put an upper limit on the maximum data rate. Since the delay spread of the channel in the worst case, 1.651 ns (Table (5)), is well within the maximum symbol period i.e. 5 μ s (200 Kbps) there will be no degradation due to ISI. Considering the worst case of the delay spread and keeping the 50% safety margin the maximum data rate of 300Mbps could be used without the use of a pulse shaper, however the system needs an equalizer since it exceeds the coherence bandwidth.

3 Measurement through Vector Network Analyzer

Channel estimation for a short range wireless system could also be done in the frequency domain with the help of a Vector Network Analyzer (VNA). The system is first calibrated with the same cables and circuitry as used by the delay domain measurements. The output of the VNA is imported into Matlab for further processing. Scattering parameters (S21) have been computed from the complex data stored in the computer. The complex channel frequency response H_n , is given by $H_n = H(f_{start} + nf_{inc})$, where f_{start} and f_{inc} are the start and increment frequencies [7].

The increment frequency has been set to 25 MHz (Sweep Bandwidth/N where N (N = 358) is the number of discrete frequency points). To compute the complex channel impulse response the inverse fast fourier transform (IFFT) is obtained from the channel frequency response (measured through VNA) for comparison with the results obtained in the delay domain [7].

The analysis of the frequency spectrum of the transmitted and received signal in the case of monopole and Vivaldi as computed in the delay domain, are compared with the spectrum obtained through VNA and is shown in Figures (16) and (17). The results obtained through VNA measurement confirm the RMS delay values obtained in Section (2.2).

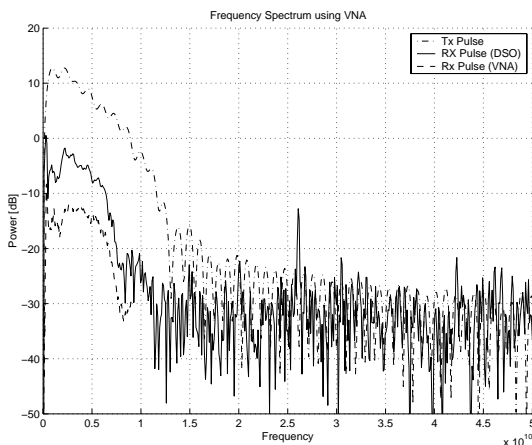


Figure 16: VNA Measurement for Vivaldi antenna

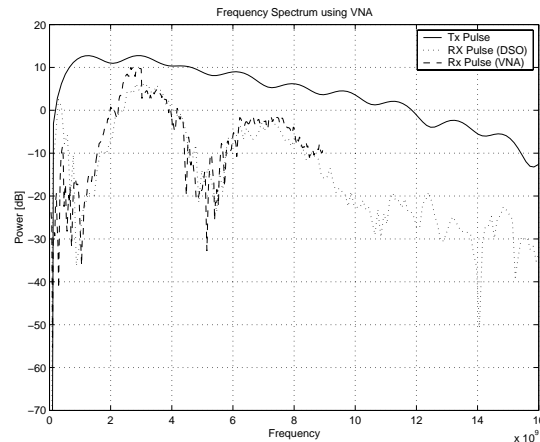


Figure 17: VNA measurements for Monopole antenna.

4 Noise and Interference

The effect of noise and interference has been considered in detail in the frequency band of 2.45 MHz. The effect of noise in the unlicensed band like 2.4 GHz ISM is important because many service providers and wireless devices operate in this band so the effect of interferes has to be considered.

To measure the effect of various noise sources a multiple set of readings have been taken in different operating environment i.e. Lab etc. The measurement setup consists of a Spectrum Analyzer (Hewlett Packard 8593) with two set of antennas: one for directional measurement (patch antenna) and another for non directional noise sources like (dipole antenna). The plots are obtained through peak and hold function.

The following observations are made, one of the major source of noise are the microwave ovens. The effect has been picked up by both the antennas within a distance of one meter. The results show a peak of 6 dB at 2.45 MHz, when a directional patch antenna is used and 11.2 dB when non directional dipole antenna is used as show in Figure (18). The interference was observed in the band around 2.4 GHz with frequency hopping (spikes) in the whole bandwidth. Some observations could be made through the acquired data i.e. the random short pulse in the band around 2.4 GHz which are not repetitive indicates the presence of wide band noise that could increase the noise floor of the system. This could create problem for devices operating on frequency hopping techniques like Bluetooth. The narrow band noise peak is observed at 2.4 GHz and this is because of the microwave operating in this band. The reason for having a higher value in case of omni directional antenna is because of the fact that it is capable of picking more multipath.

The other noise sources which are investigated are the laptop computers and the mobile phones. No credible evidence of any interference caused by these devices was observed in 2.45 GHz band.

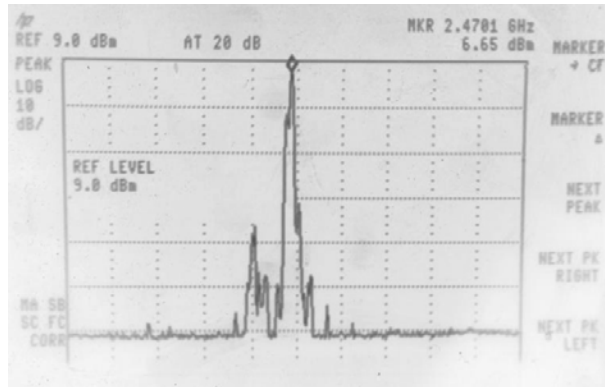


Figure 18: Spectrum Analyzer at 2.4 GHz band

5 Conclusion

In this paper we presented the channel parameters for small transceivers called 'specks'. The first prototype version of 'Specknet' has a data rate fixed at 200Kbps. With this data rate using Manchester encoded data the transmission bandwidth of the signal is well within the coherence bandwidth of the channel. This indicates that no equalization is needed at the receiver. Secondly, there will be no degradation because of ISI (Inter symbol interference) as the delay spread of the channel Table (5) and (6) is in the order of fraction of nsec as compared to the pulse duration. The channel is considered to be a flat faded channel. This will result in more power to be sent to compensate for the deep fade. The paper also presented the possible noise sources in the band of interest especially that caused by microwave ovens.

The future research will be based on designing statistical channel models based on the findings of this paper. A comprehensive link budget analysis based on the hardware used in the transceiver along with error curves could be added in future.

6 Acknowledgements

The author gratefully acknowledges support from the SHEFC (Scottish Higher Education Funding Council) and the input of Specknet Consortium members [9].

References

- [1] Constantine Balanis, "Antenna Theory", 3rd Edition 2005. pp 44-47. ISBN 0-471-66782-X
- [2] R.M.Buehrer, A.Safaai-jazi,W.A.Davis, and D. Sweeney, " Characterization of the UMB Channel," Proc.IEEE Conference on Ultra Wideband Systems and Technologies, pp.26-31,Reston, VA, November 2003.
- [3] Liberti, J.C.; Rappaport, T.S, "Statistics of shadowing in indoor radio channels at 900 and 1900 MHz", Military Communications Conference, 1992. MILCOM '92, Conference Record', Communications.

- [4] Brian M. Donlan, Swaroop Venkatesh, Vivek Bharadwaj, R. Michael Buehrer, and Jiann-An Tsai. "The Ultra Wideband Indoor Channel", Vehicular Technology Conference, 2004. VTC 2004-Spring. 2004 IEEE 59th, Vol.1, 17-19 May 2004 Page(s):208 - 212 Vol.1.
- [5] David M. Pozar, "Microwave Engineering", 2nd Edition 1998. pp 19-21. ISBN 0-471-17096-8
- [6] T.S.Rappaport, "Wireless Communication principles and practice" – 2nd Edition. 2002. Singapore: Pearson Education, 2002, Ch. 4, pp. 107-109, pp. 135-144, Ch. 5, pp. 190-205.
- [7] A.M.Street, L.Lukama and D.J.Edwards. "Use of VNAs for wideband propagation measurement", Communications, IEE Proceedings-Volume 148, Issue 6, Dec. 2001 Page(s):411 - 415 Digital Object Identifier 10.1049/ip-com: 20010639.
- [8] Moe Z. Win, Robert A. Scholtz, "Characterization of Ultra-wide bandwidth wireless indoor channel: A communication-theoretic view", IEEE Journal on selected areas in communication, vol 20, Dec 2002, pp. 1613-1614.
- [9] www.specknet.org